ELSEVIER

Determination of K, Ar, Cl, S, Si and Al flare abundances from RESIK soft X-ray spectra

J. Sylwester [a,*], B. Sylwester [a], E. Landi [b], K.J.H. Phillips [c], V.D. Kuznetsov [d]

[a] *Space Research Centre, Polish Academy of Sciences, ul. Kopernika 11, PL-51-622 Wroclaw, Poland*
[b] *Artep, Inc. at Naval Research Laboratory, USA*
[c] *Mullard Space Science Laboratory, University College, London, UK*
[d] *IZMIRAN, Russian Academy of Sciences, Troitsk, Russia*

Abstract

The RESIK is a high sensitivity, uncollimated bent crystal spectrometer which successfully operated aboard Russian *CORONAS-F* solar mission between 2001 and 2003. It measured for the first time in a systematic way solar soft X-ray spectra in the four wavelength channels from 3.3 Å to 6.1 Å. This range includes characteristic strong lines of H- and He-like ions of K, Ar, Cl, Si, S and Al in the respective spectral channels. A distinguishing feature of RESIK is its possibility of making reliable measurements of the continuum radiation in flares. Interpretation of line and the continuum intensities observed in vicinity of respective strong lines provides diagnostics of plasma temperature and absolute abundances of K, Ar, Cl, S, Si and Al in several flares. We analyzed the observed intensities of spectral lines and the nearby continuum using the CHIANTI v5.2 atomic data package. A specific, so-called "locally isothermal" approach has been used in this respect allowing us to make not only flare-averaged abundance estimates, but also to look into a possible variability of plasma composition during the course of flares.
© 2007 COSPAR. Published by Elsevier Ltd. All rights reserved.

Keywords: Solar physics; X-ray flares; Spectroscopy; Abundances

1. RESIK bent crystal spectrometer

The RESIK consists of two double-channel X-ray spectrometers equipped with bent crystals, a design similar to the BCS spectrometers aboard *SMM* and *Yohkoh*. RESIK was designed to observe hot solar plasmas. It was included in the scientific payload of the Russian solar satellite mission *CORONAS-F*. The detailed description of the RESIK instrument, its operation and calibration are presented in the paper by Sylwester et al. (2005). Here we summarize a number of instrument characteristics important for the present study. The nominal wavelength coverage of RESIK was 3.40–6.05 Å. This range contains several spectral features useful for the X-ray plasma diagnostics. The observed line intensities can be used in order to study the physical conditions in the flaring plasma as well as to investigate its relative (element-to-element) composition. Inclusion of the continuum, also reliably measured, allows us to measure the absolute (relative to hydrogen) abundances, as substantial contribution to the continuum comes from bremsstrahlung emission. In the RESIK spectra one can find lines belonging to the elements with substantially different values of FIP: from 4.34 eV (K) to 15.75 eV (Ar). Other lines are identified by Sylwester et al. (2006) and Kepa et al. (2006). They include the triplets of He-like ions (K XVIII, Ar XVII, Cl XVI and S XV) as well as lines corresponding to $(n > 3) \to (1)$ transitions in Si and Al.

2. Observed spectra and new abundance analysis approach

For purpose of the present analysis we have selected seven typical flares, well observed by RESIK. The flares

---

* Corresponding author.
  E-mail address: js@cbk.pan.wroc.pl (J. Sylwester).

selected represent short and longer duration events seen on the disk and/or at the limb. All flares (cf. Table 2) were observed early in 2003, when the instrument settings were optimized. We have carefully calibrated the observed spectra, establishing an absolute wavelength scale and determining the absolute spectral photon fluxes. We incorporated all known corrections which essentially remove the instrumental fluorescence radiation from the RESIK bent crystals material. This leads us to believe that the level of the continuum seen in the longer wavelength channels of RESIK represents uncontaminated solar continuum. For the two shorter wavelength bands, the contribution of the fluorescence to the measured spectra was found not to be a problem as it amounts to less than one percent. In Fig. 1, we have presented the spectrum integrated over the entire flare on 2003 February 22 at 09:30 UT selected for the analysis of the absolute elemental abundances. The six wavelength intervals chosen for the abundance determination of individual elements are indicated. Respective lines making contribution to individual bands' fluxes are listed in Table 1 together with the line identification and appropriate transitions given.

In the analysis, we have used a novel "locally isothermal" (LI) approach in order to separate the impact of abundance variability from the temperature (multitemperature-DEM) effects on the spectra as much as possible. In the LI approach we make "implicit use" of somewhat similar temperature dependence of the line and the nearby continuum emission functions in the region of the effective line formation. This similarity causes the abundance effects to dominate over DEM effects in the Line-to-Continuum (L/C) ratio variability.

Our non-standard determination technique is based on converging iterative scheme, where we start from the measured value of a total, band-integrated flux, including the lines of the element of interest, the lines from the other elements contributing to the band flux and a substantial part of near-by continuum. A counterpart, theoretically predicted fluxes in the same selected wavelength band depend on the assumed plasma temperature, emission measure and the composition. For purposes of the spectral synthesis task, we pre-calculated an extensive ~10 GB database consisting of a grid of theoretical spectra, with $\delta\lambda = 0.001$ Å, for 101 temperatures between 1 and 100 MK, for six elements: K, Ar, Cl, S, Si and Al, and for 41 abundance values of each element. The calculations were based on CHIANTI v5.2 spectral code, a part of *SolarSoft* (Dere et al., 1997). The important free-free and free-bound processes have all been included in the calculations of the continuum. As checked by Chifor et al. (2006) the continuum calculations following from CHIANTI are in very good agreement (few percent) with the earlier results of Mewe et al. (1985). As these two sets of calculations depend on independent approximations for the basic atomic cross-sections, such a good agreement increases our confidence in derived values of the abundances discussed in the present study. In the process of finding the optimum fit between the observed and calculated spectrum (for each band analyzed separately), we build-up a two-dimensional array of the χ^2 values in the following way:

(1) We adopt a pair of values for the abundance A_{El} of the considered element and the plasma temperature T.
(2) Calculate the emission measure EM from the observed band-integrated flux and respective CHIANTI-based band-integrated flux.
(3) Use this EM, to predict the "calculated" spectral shape for each individual bin within the band, including all lines and the continuum and adopting known instrumental line shape.
(4) Calculate the normalized χ^2 of the difference between the observed and calculated spectra.
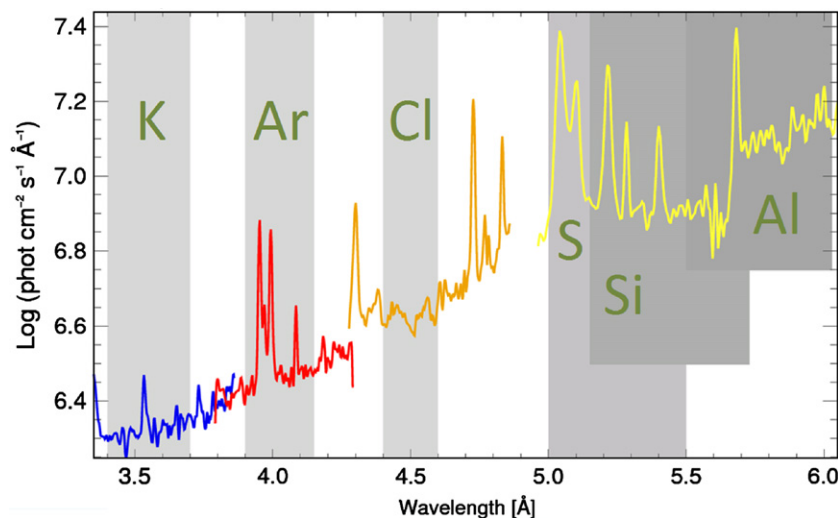

Fig. 1. An example of a calibrated RESIK spectrum. This spectrum was accumulated over entire 2003 February 22 flare which took place around 09:30 UT. In gray, several spectral bands are marked, selected to study the absolute abundance of indicated respective elements. For the color version of this and the other figures, visit http://www.cbk.pan.wroc.pl/publications/2006/determination.html.

Table 1
Main lines used for the abundance study

Band range (Å)	Wavelength (Å)	Line	Ion	Transition
K	3.53	w	K XVIII	$1s^{2\,1}S_0–1s2p^1P_1$
3.40–3.70	3.55	x,y	K XVIII	$1s^{2\,1}S_0–1s2p^3P_{1,2}$
	3.57	z	K XVIII	$1s^{2\,1}S_0–1s2s^3S_1$
	3.53–3.60	sat	K XVII	*satellites* to the above
Ar	3.95	w	Ar XVII	$1s^{2\,1}S_0–1s2p^1P_1$
3.90–4.15	3.97	x,y	Ar XVII	$1s^{2\,1}S_0–1s2p^3P_{1,2}$
	3.99	z	Ar XVII	$1s^{2\,1}S_0–1s2s^3S_1$
	3.95–3.99	sat	K XVII	*satellites* to the above
Cl	4.44	w	Cl XVI	$1s^{2\,1}S_0–1s2p^1P_1$
4.40–4.60	4.47	x,y	Cl XVI	$1s^{2\,1}S_0–1s2p^3P_{1,2}$
	4.50	z	Cl XVI	$1s^{2\,1}S_0–1s2s^3S_1$
	4.44–4.52	sat	Cl XV	*satellites* to the above
S	5.04	w	S XV	$1s^{2\,1}S_0–1s2p^1P_1$
5.00–5.50	5.06	x,y	S XV	$1s^{2\,1}S_0–1s2p^3P_{1,2}$
	5.10	z	S XV	$1s^{2\,1}S_0–1s2s^3S_1$
	5.04–5.21	sat	S XIV	*satellites* to the above
Si	5.22	Lyβ	Si XIV	$1s^2S_{1/2}–3p^2P_{3/2,1/2}$
5.15–5.73	5.29	5p	Si XIII	$1s^{2\,1}S_0–1s5p^1P_1$
	5.40	4p	Si XIII	$1s^{2\,1}S_0–1s4p^1P_1$
	5.40–5.57	4p sat	Si XII	*satellite* to the above
Al	5.60	Lyδ	Al XIII	$1s^2S_{1/2}–5p^2P_{3/2,1/2}$
5.50–6.03	5.74	Lyγ	Al XIII	$1s^2S_{1/2}–4p^2P_{3/2,1/2}$

(5) Repeat 1–4 for all combinations of T (101 points) and A_{El} (41 points).

The T-A_{El} calculation mesh covers the temperature range 1–100 MK with 101 logarithmically spaced intervals and A_{El} with 41 linearly spaced values, covering the range between zero and four times the respective coronal elemental abundance value (Feldman and Laming, 2000).

On the obtained χ^2 surface, we identify the position of local minimum in the T-A_{El} parameter space, and plot respective 1σ contours according to the classical approach of Bevington (1969). The example result of the described procedure is illustrated in Figs. 2 and 3.

3. The results

In Figs. 4 and 5, we show examples of time dependence of best-fit abundance determinations for two flares observed by RESIK in contiguous manner. One flare had a short rise and decay time and fell entirely within the 20 min RESIK observation window. However it was a rather faint event, and therefore the statistically reliable spectra collection time was necessarily longer for the early rise and late decay phases. The other flare was much stronger with two pronounced maxima. It was possible to study its spectral variability every few seconds. In Figs. 4 and 5, we plot the abundance values for each element together with respective $\pm 1\sigma$ uncertainties. These uncertainties represent the size of the "min(χ^2) + 1σ" contour from Fig. 3, as projected onto the abundance axis. It is worth noting that the results presented in Figs. 4 and 5 show for the first time the plasma composition variability *during* flares, as

determined from spectroscopic data. Examination of these Figures and similar plots constructed for the other flares studied, allows us to draw a number of conclusions.

- For many events the plasma composition is approximately constant in time.
- For some events like 2003 February 22, A_{Ar} appears to anticorrelate with A_K; these two elements have the largest FIP contrast among those studied.
- For the events shown in Figs. 4 and 5, it is highly improbable that the time variability pattern observed occurs by chance, and therefore, we conclude that the plasma composition changes take place during flares.

If the above conclusions are confirmed in a following larger study covering many tens of flares observed by RESIK, the physical consequences are expected to be profound for considerations concerning the origin (source) of matter contributing to soft X-ray flaring plasma. It is possible, that such matter may be characterized by a highly non-uniform composition probably caused by plasma-magnetic field differentiation mechanisms acting selectively on semi-ionized gas over longer periods.

Based on the observed composition variability pattern for the analyzed flares, it was possible to determine seven flare-averaged plasma abundance sets for the six elements studied. These averaged values are given in Table 2, together with formal $\pm 1\sigma$ uncertainties. The uncertainties were calculated taking into account the scatter around the mean value. The uncertainties are larger for cases where the abundance appears to be time dependent. It should be noted that we made all possible efforts in order to remove
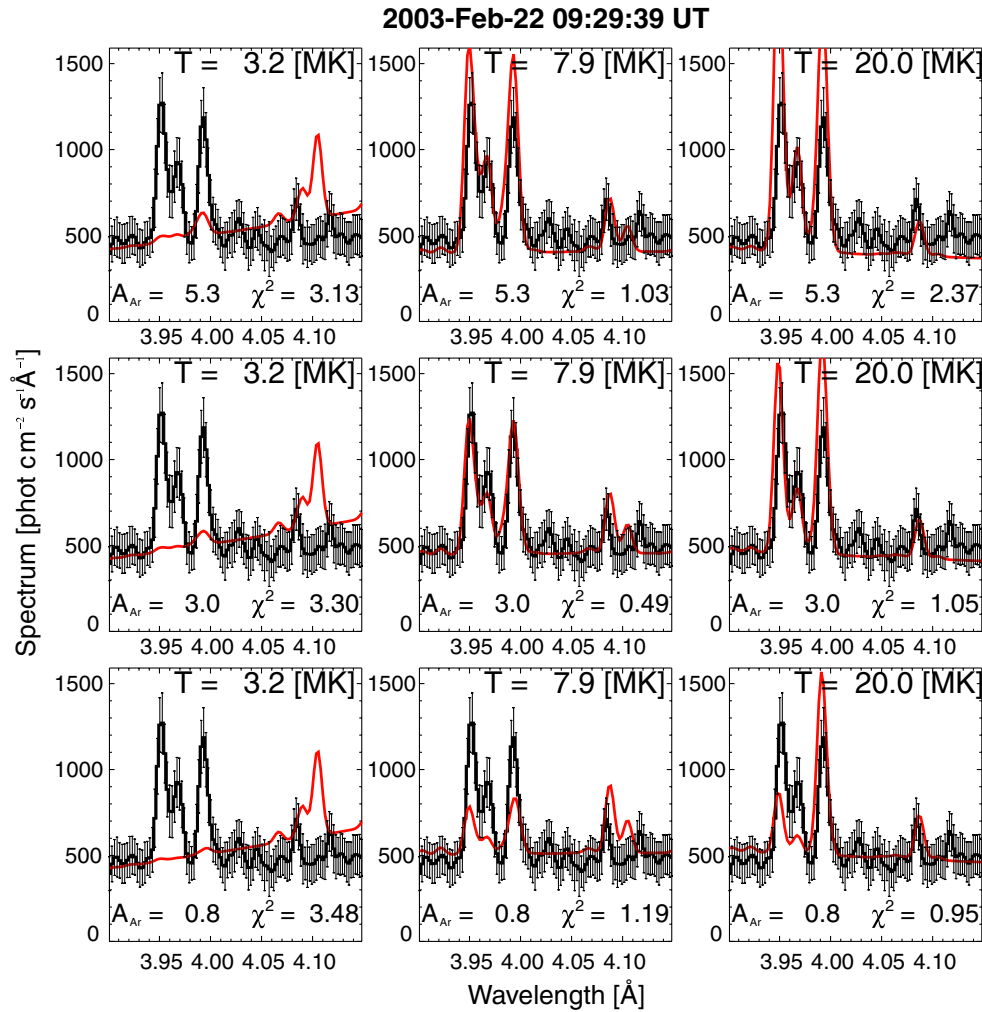
2003-Feb-22 09:29:39 UT

Fig. 2. Nine examples of the fits between observed (histogram) and synthetic spectra for the maximum phase of the flare on 2003 February 22. In each row, the abundance of the element of interest (Ar) is kept constant and the plasma temperatures correspond to three different values. In each column, the plasma temperature is constant and the abundance of Ar is set to three different values. In the central panel, the optimum fit is shown, characterized by the smallest value of χ^2 parameter. Such an optimum fit has been obtained for each of the spectra recorded throughout the flare.
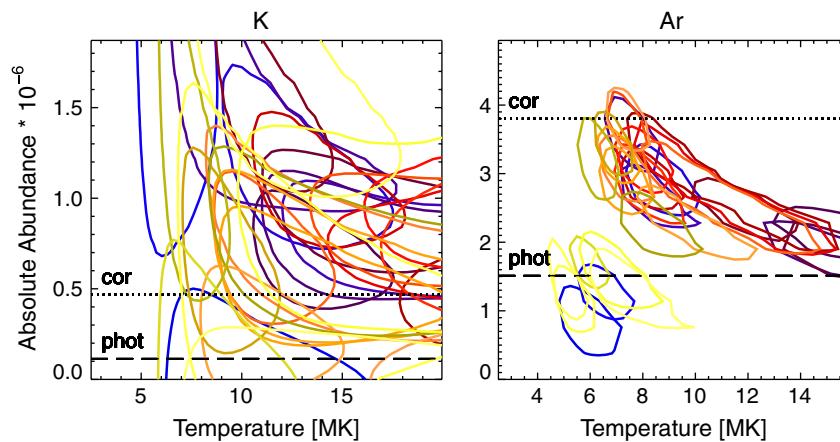

Fig. 3. Left: contours of "min(χ^2) + 1σ" for potassium (2003 February 22, 09:30 UT flare). Shades of the contours are dark for the flare rise phase, coming lighter towards the decay phase. Right: a corresponding diagram shown for more abundant element argon. Here the "min(χ^2) + 1σ" contours are more compact which indicates that respective abundance uncertainties are much smaller. The "phot" and "cor" horizontal lines designate the photospheric and coronal abundance levels as taken from Asplund et al. (2005) and Feldman and Laming (2000), respectively.
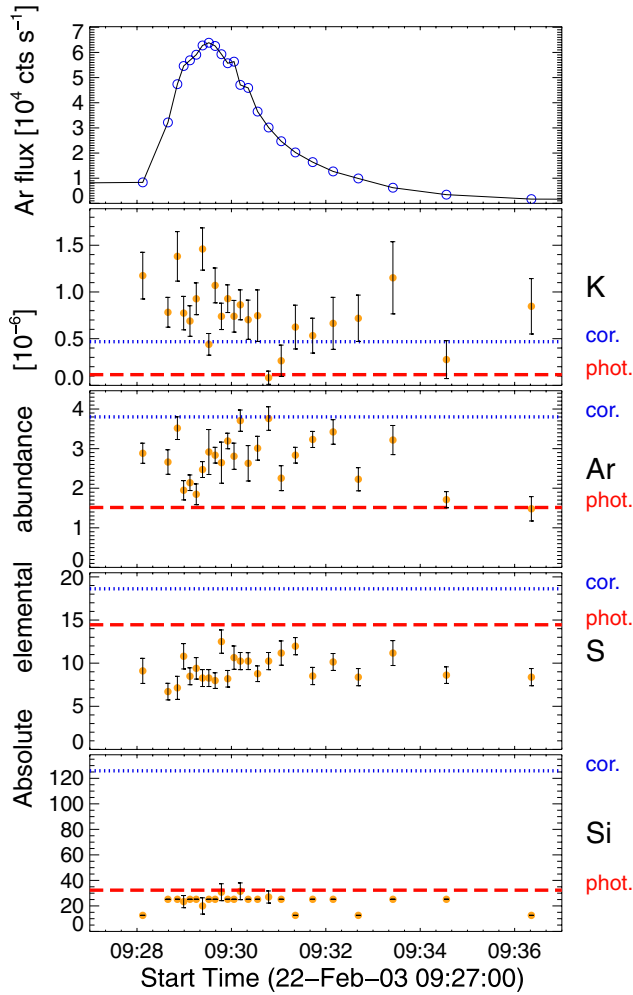
Fig. 4. Time dependence of derived flare abundances for a fast evolving flare on 2003 February 22. In the upper part, the flare flux as seen in the Ar spectral band is plotted. The uncertainties drawn correspond to the vertical extension of the iso-contours shown in Fig. 3. Respective coronal and photospheric abundance levels are given for each element as dotted and dashed lines, respectively.

Fig. 5. Time dependence of derived flare abundances for a "double" flare of 2003 January 9. In the upper part, the flare flux as seen in the Ar spectral band is plotted. Respective coronal and photospheric abundance levels are given for each element as dotted and dashed lines, respectively.

all known instrumental effects in the data reduction. The largest instrumental component of the order of 20% of the measured continuum level (called pedestal) has been removed from channel 3 and 4. The origin of this pedestal, modeled numerically and calibrated in-flight, was a solar X-ray induced fluorescence. The results of the present abundance study should not be affected strongly by the amount connected to this 20% uncertainty. However it may contribute to the presence of a systematic bias in the abundance determinations for S, Si and Al. The work is in progress in order to further narrow the amount of such bias.

4. Summary and conclusions

In this study we present analysis of RESIK bent crystal spectrometer soft X-ray spectra for seven well-observed flares. The novel nature of the spectral analysis applied, as well as unprecedented quality of the spectra measured, have allowed us to study time-variability of absolute ele-
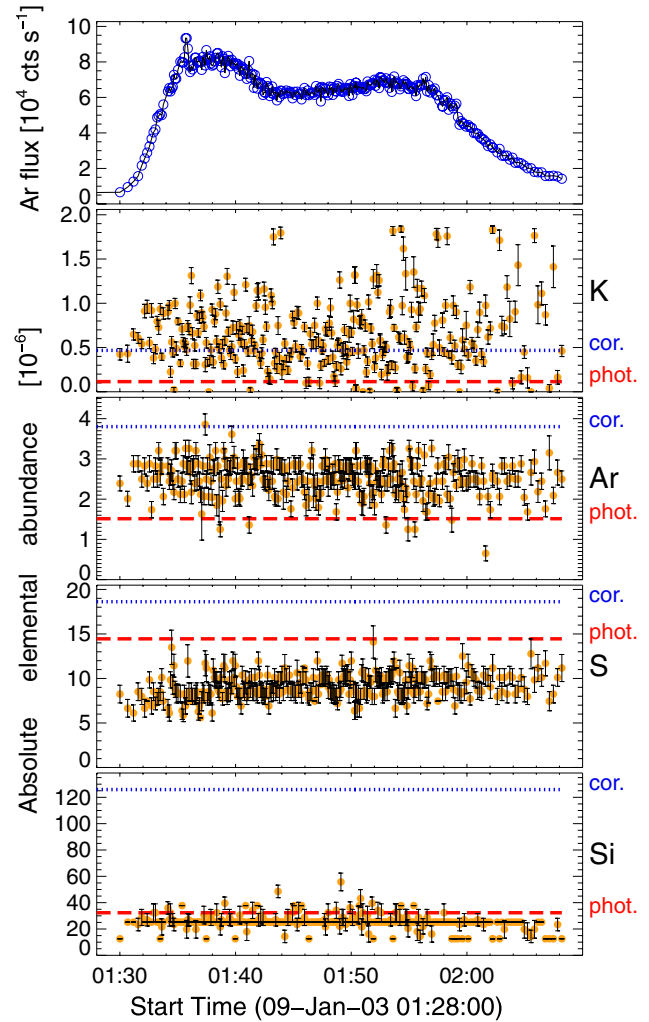
mental composition for the following elements: K, Ar, Cl, S, Si and Al. The results shown in Figs. 4 and 5 indicate for a possible changes in flaring plasma composition as the flare progress. The flare-averaged composition for seven analyzed flares (presented in Table 2) is seen to vary from event-to-event. The amplitude of variability is the largest for the low-FIP elements like potassium. Derived average abundances of sulphur and silicon are significantly below, at the level of ($\sim$60%) of the photospheric values taken from Asplund et al. (2005). Abundances of Ar are between the photospheric and coronal (Feldman and Laming, 2000) values, while for potassium and aluminum the derived values are above respective coronal levels. Notwithstanding of a careful analysis of the instrumental fluorescence contribution, there is still a possibility of some uncounted contamination of fluorescence in the RESIK channel where S, Si and Al lines are observed. Work is in progress and we hope to present completely unbiased estimates for these elements in the subsequent extended study following the outline presented here.

Table 2
Average absolute flare abundances [10^{-6}]

FIP (eV) $\Rightarrow$		4.34	15.76	12.97	10.36	8.15	5.99
Flare$\Downarrow$ Element $\Rightarrow$		K	Ar	Cl	S	Si	Al
2003-Jan-04 06:30		0.49	2.24	0.52	8.73	17.4	12.2
B9.2	S23 E50	±0.4	±0.5	±0.2	±1.5	±6.0	±6
2003-Jan-07 07:50		0.51	2.24	0.35	10.1	30.5	7.2
M1.0 S24	E08	±0.4	±0.6	±0.3	±1.4	±17	±9
2003-Jan-07 23:30		0.68	2.40	0.40	9.46	18.7	11.3
M4.9	S11 E08	±0.5	±0.9	±0.3	±1.5	±6.4	±10
2003-Jan-09 01:39		0.64	2.51	0.30	9.13	25.3	6.7
C9.8	S09 W25	±0.4	±0.5	±0.3	±1.4	±5.6	±8
2003-Jan-21 15:26		0.42	2.74	0.35	11.0	26.0	7.8
M1.9	S07 E90	±0.3	±0.8	±0.4	±1.4	±8.5	±9
2003-Jan-25 18:55		0.71	2.89	0.31	9.93	25.6	9.3
C4.4	N13 W27	±0.5	±1.0	±0.3	±3.6	±27	±8
2003-Feb-22 09:30		0.77	2.46	0.30	9.46	22.3	12.4
C5.8	N16 W05	±0.4	±0.8	±0.2	±1.7	±5.7	±7
A_{El} photospheric[a] $\Rightarrow$		0.115	1.51	0.170	14.45	32.36	2.69
A_{El} coronal[b] $\Rightarrow$		0.468	3.80	0.316	18.62	125.9	10.96

[a] From Asplund et al. (2005).
[b] From Feldman and Laming (2000).

Acknowledgements

References

Asplund, M., Grevesse, N., Sauval, A.J. Cosmic abundances as records of stellar evolution and nucleosynthesis. ASP Conf. Ser. 336, 25–38, 2005.

Bevington, P.R. Data Reduction and Error Analysis for the Physical Sciences. McGraw-Hill Book Company, New York, 1969.

Chifor, C., Del Zanna, G., Mason, H.E., Sylwester, J., Sylwester, B., Phillips, K.J.H. A benchmark study for CHIANTI based on RESIK solar flare spectra. Astron. Astrophys. 462, 323–330, 2006.

Dere, K.P., Landi, E., Mason, H.E., & others, An Atomic Database for Emission Lines, Astron. Astrophys. Sup. 125, 149–173, 1997.

Feldman, U., Laming, J.M. Elemental abundances in the upper atmospheres of the Sun and stars: update of observational result. Phys. Scr. 61, 222–252, 2000.

Kepa, A., Sylwester, J., Sylwester, B., Siarkowski, M., Phillips, K.J.H., Kuznietsov, V.D. Observations of $1s^2$-1s np and 1s-np lines in RESIK soft X-ray spectra. Adv. Space Res. 38, 1534–1537, 2006.

Mewe, R., Lemen, J., van den Oord, G.H. J. Calculated X-radiation from optically thin plasmas. VI - Improved calculations for continuum emission and approximation formulae for nonrelativistic average Gaunt factors. Astron. Astrophs. Sup. 65, 511–536, 1985.

SolarSoft – http://sohowww.nascom.nasa.gov/solarsoft/.

Sylwester, J., Gaicki, I., Kordylewski, Z., et al. RESIK: A bent crystal X-ray spectrometer for studies of solar coronal plasma composition. Sol. Phys. 226, 45–72, 2005.

Sylwester, B., Sylwester, J., Siarkowski, M., & 5 others, Lines in the range 3.2–6.1 Å observed in RESIK spectra, Adv. Space Res. 38, 1490–1493, 2006.